Thermal and Rheological Studies on the Molecular Composition and Structure of Metallocene- and Ziegler–Natta-Catalyzed Ethylene–α-Olefin Copolymers

P. STARCK, A. MALMBERG,* B. LÖFGREN

Polymer Science Centre, Helsinki University of Technology, Innopoli B2, P.O. Box 356, FIN-02151 Espoo, Finland

Received 2 January 2001; accepted 6 March 2001

ABSTRACT: The relationship between the molecular structure and the thermal and rheological behaviors of metallocene- and Ziegler–Natta (ZN)-catalyzed ethylene copolymers and high-density polyethylenes was studied. Of special interest in this work were the differences and similarities of the metallocene-catalyzed (homogeneous) polymers with conventional coordination-catalyzed (heterogeneous) polyethylenes and low-density polyethylenes. The short-chain branching distribution was analyzed with stepwise crystallization by differential scanning calorimetry and by dynamic mechanical analysis. The metallocene copolymers exhibited much more effective comonomer incorporation in the chain than the ZN copolymers; they also exhibited narrower lamellar thickness distributions. Homogeneous, vanadium-catalyzed ZN copolymers displayed a very similar comonomer incorporation to metallocene copolymers at the same density level. The small amplitude rheological measurements revealed the expected trend of increasing viscosity with weight-average molecular weight and shear-thinning tendency with polydispersity for the heterogeneous linear low-density polyethylene and very-low-density polyethylene resins. The high activation energy values (34–53 kJ/mol) and elevated elasticity found for some of our experimental metallocene polymers suggest the presence of long-chain branching in these polymers. This was also supported by the comparison of the relationship between low shear rate viscosity and molecular weight. © 2002 John Wiley & Sons, Inc. J Appl Polym Sci 83: 1140–1156, 2002

Key words: metallocene catalysts; Ziegler–Natta; polyethylene (PE); short-chain branching; long-chain branching; rheology

INTRODUCTION

The major advantage of metallocene catalysts over conventional Ziegler–Natta (ZN) catalysts is the possibility of the synthesis of ethylene copolymers with a narrow molecular weight distribution (MWD) and narrow comonomer distribution (CD).[1] Most metallocene copolymers have a homogenous short-chain branching (SCB; branch frequency the same for all molecules), whereas the ZN copolymers are heterogeneous; that is, the branch frequency varies from molecule to molecule.[2] The controlled molecular structure of the metallocene polyethylenes leads to many desirable properties, including superior mechanical properties compared with polyolefins made with standard ZN catalyst technology.[3,4] Many extensive studies have been carried out to understand the structure, morphology, and property relationships of the various polyethylenes. Temperature

Correspondence to: P. Starck (paul.starck@innopoli.fi).
* *Present address:* Borealis Polymers Oy, P.O. Box 330, FIN-06101 Porvoo, Finland.

Journal of Applied Polymer Science, Vol. 83, 1140–1156 (2002)

DOI 10.1002/app.10152

rising elution fractionation (TREF) has widely been used to measure CD in low-density polyethylene (LDPE), Ziegler–Natta linear low-density polyethylene (ZN LLDPE), and Ziegler–Natta very-low-density polyethylene (ZN VLDPE).[4,5] Recently, TREF studies on metallocene-type polyethylenes were also announced.[6] Differential scanning calorimetry (DSC) has been used over the last decade to study molecular segregation based on molecular weight and chemical composition during crystallization from the melt.[7–15] These methods, which correlate melting temperature (T_m) with SCB, have been called the stepwise isothermal segregation technique,[7] step crystallization (SC),[8,12] thermal fractionated crystallization,[9] DSC fractionation,[10] and successive self-nucleation/annealing.[14]

Dynamic mechanical analysis (DMA) is another technique that is sensitive to the structural heterogeneity of polyethylene because the relaxation behavior is strongly influenced by variables such as crystallinity, lamellar thickness, and interfacial structure.[16] Normally, three relaxations are observed, identified as α, β, and γ in order of decreasing temperature. The β-transitions occurring between about -40 and 20°C[17–20] have yielded the best information for studies of branch distribution and branch-type influence.

The processability of polymeric materials is closely related to the rheological properties in the molten state. SCB strongly affects solid-state properties but has virtually no effect on melt rheology. For instance, Kalyon et al.[21] concluded that the differences in rheological behavior caused by the comonomer type in ethylene–α-olefin copolymers were rather insignificant. Long-chain branching (LCB), such as that appearing in LDPE has, however, long been known to strongly affect melt rheological properties.[22,23] The absence of LCB in linear low-density polyethylene (LLDPE) has, for a long time, been classed as a fundamental molecular difference between LLDPE and LDPE. This has been true both for ZN LLDPEs and metallocene LLDPEs. LDPE shear thins extensively in the shear rate range common to most extrusion processes (80–8000 1/s), but the viscosity of LLDPE is notably less sensitive to shear in this shear rate range and thus exhibits a significantly higher shear viscosity (η) in extrusion than a LDPE of similar melt flow rate (MFR). Heterogeneous LLDPE, therefore, needs more motor power, develops higher melt temperatures in processing than LDPE, and behaves in a very similar way to high-density polyethylene (HDPE) in the molten state. Although the homogeneous LLDPEs and HDPEs have better physical properties than heterogeneous LLDPEs and HDPEs, they are even more difficult to process as a result of their narrow MWD. Several articles,[2,3,24–38] however, have reported that certain classes of metallocene catalysts can produce polymers with controlled amounts of LCB, which leads to both excellent processability and superior mechanical properties.

In this study, we employed SCs by DSC and studies of the β relaxations by DMA to characterize the CD of both homogeneous and heterogeneous copolymers. The weight-average molecular weight (M_w) and polydispersity [M_w/number-average molecular weight (M_n)] of these polymers was studied with size exclusion chromatography (SEC), and the melt flow properties were studied by dynamic rheological measurements. The main objective of our work was to elucidate the structure–property relationships of a wide range of commercial and experimental metallocene polyethylenes and to discuss their influences on the thermal and rheological behavior of these polymers and that some of the rheological differences of the metallocene-catalyzed polymers are due to the presence of LCB. Of special interest in this work were the differences and similarities between the conventional coordination-catalyzed polyethylenes and LDPEs.

EXPERIMENTAL

Materials

The polymers studied consisted of commercial ZN-catalyzed LLDPE, very-low-density polyethylene (VLDPE), and HDPE polymers; LDPE polymers; and both experimental and commercial metallocene-catalyzed polyethylenes synthesized with various metallocene catalysts. Some of their characteristic features are given in Tables I and II.

Polymer LD-1 was a thoroughly characterized polymer, studied in an IUPAC round-robin work.[39] Polymer LD-2 was a narrow-MWD LDPE film-grade material, polymer LD-3 was a broad-MWD LDPE extrusion coating material, and polymer LD-4 was a broad-MWD LDPE wire and cable material; all were made in a high-pressure autoclave process.

The ZN LLDPE and VLDPE polymers studied in this work were made by different producers in the gas phase (ZNLLD-5 and ZNVLD-8), in solu-

Table I Characteristics of Polymers Used in This Study

Sample	Comonomer Type	Comonomer wt %	Density (kg/m^3)	T_m (°C)	Crystallinity X_c (%)	Tan δ (°C/peak height)	E'' (°C)
LD-1	—	—	922	113.3	34	−26	−27
LD-2	—	—	922	111.4	32	n.d.	n.d.
LD-3	—	—	915	105.4	32	n.d.	n.d.
LD-4	—	—	920	113.4	36	n.d.	−21
ZN LLD-5	C4	7.2	920	122.0	35	−24/0.05	−33
ZN VLD-6	C4	10.6	912	119.0	24	−27/0.06	−35
ZN VLD-7	C4	11.2	899	117.3	21	—	—
ZN VLD-8	C4	12.1	908	119.4	30	−32/0.07	−58
ZN VLD-9	C4	16.8	888	70.4	13	−30/0.29	−47
ZN VLD-10	C8	13.5	912	125.0	26	−25/0.09	−38
ZN HD-11	C4	1.3	—	128.4	57	—	—
ZN HD-12	—	—	959	134.9	60	—	—
ZN HD-13	—	—	958	134.3	70	—	—
me LLD-14	C4	5.4	923	115.3	36	n.d.	−18
me LLD-15	C6	7.4	918	112.3	37	n.d.	(−25)
me HD-16	—	—	952	132.5	59	—	—
me VLD-17	C8	16.6	907	91.4	19	−24	−40
me VLD-18	C8	21.0	898	95.6	21	−9/0.28	−43
me VLD-19	C4	13.8	899	85.3	20	−19/0.21	−35
me VLD-20	C4	22.4	881	60.0	7	−20/0.21	−43
me VLD-21	C4	10.4	905	96.5	23	−7/0.18	−33
me VLD-22	C4	15.1	895	87.4	20	−22/0.23	−42
me HD-23	—	—	n.a.	131.9	63	n.d.	n.d.
me MD-24	C6	2.5	937	123.3	46	n.d.	n.d.
me MD-25	C6	2.5	936	121.5	46	n.d.	n.d.
me MD-26	C6	1.7	939	124.5	50	n.d.	n.d.
me LLD-27	C6	5.5	927	115.3	38	—	—

n.d. = not detected.
(−25) = weak detection.
— = not analyzed.

tion (ZNVLD-9 and ZNVLD-10), and in a modified high-pressure process (ZNVLD-6 and ZNVLD-7). Polymer ZNVLD-9 was made with a vanadium (V) catalyst. The HDPE polymers made with ZN catalysts (ZNHD-11 and ZNHD-13) were both bimodal. The unimodal ZNHDPE-12 was synthesized with a chromium (Cr) catalyst.

Polymers meLLD-14 to meLLD-22 were commercial grades from various suppliers, synthesized with metallocene catalysts. These polymers were expected to be linear (non-LCB) with the exception of meVLD-18, which was synthesized with the Dow (Freeport, TX) constrained geometry catalyst (CGC). The catalyst system used for the metallocene copolymer meVLD-17 was not confirmed. Polymers meHD23 to meLLD27 were experimental lab scale polymers produced in slurry polymerizations with methylaluminoxane (MAO)-activated metallocene catalysts. Polymer meHD-23 was polymerized with *rac*-[ethylenebis(1-*tert*-butyldimethylsiloxy)indenyl)]zirconiumdichloride, meMD-24 with *rac*-[ethylenebis(tetrahydroindenyl)]zirconiumdichloride, meMD-25 with *rac*-[ethylenebis(2-*tert*-butyldimethylsiloxy)indenyl]-zirconiumdichloride, and meMD-26 and me-LLD27 with *rac*-[ethylenebis(indenyl)]zirconiumdichloride. Details of the polymerization have been reported elsewhere.[32,37]

Characterization

The MFRs at 190°C and the densities of the resins were measured according to ISO-1133 (2.16 or 21.6 kg weights) and ISO-1183, respectively. The contents of the comonomers (butene, hexene, and octene) in the polymers was determined by ^{13}C-NMR (Jeol GSX, 400 MHz, Tokyo, Japan) at 100 MHz in 1,2,4-trichlorobenzene at 140°C.

Table II Rheological and Molecular Weight Data of the Investigated Polymers

Sample	MFR_2 (g/10 min)	MFR_{21} (g/10 min)	M_w (kg/mol)	MWD	η^* at 0.02 rad/s 190°C (Pa)	G' (G'' = 2000 Pa; Pa)	G' (G'' = 5000 Pa; Pa)	G' (G'' = 10,000 Pa; Pa)	E_a (kJ/mol)
LD-1	2.2	—	206[a]	8.3	6200	650	2500	6600	55
LD-2	4.0	—	120[a]	4.8	3200	520	2200	6000	54
LD-3	8.0	—	715[a]	33	3350	960	3200	7720	48
LD-4	0.3	—	785[a]	38	44,500	780	2900	7800	59
ZN LLD-5	1.0	—	127	5.1	11,800	510	1590	3770	—
ZN VLD-6	0.95	—	126	4.3	21,600[b]	510	1600	3900	—
ZN VLD-7	12	—	51	3.2	2280[b]	500	1700	4200	—
ZN VLD-8	0.82	—	126	4.2	39,900[b]	750	2150	4800	—
ZN VLD-9	3.5	—	68	1.9	3140[b]	100	430	1270	—
ZN VLD-10	3.3	—	88	3.8	6400[b]	410	1380	3500	—
ZN HD-11	—	—	300	30	224,000	—	3770	8000	—
ZN HD-12	—	1.9	400	11.5	410,000	—	—	8440	25
ZN HD-13	0.25	25	240	23.3	60,000	1080	3100	7020	—
me LLD-14	2.8	—	76	2.2	2600	68	310	900	27
me LLD-15	3.2	49.7	86	2.0	2420	66	310	970	30
me HD-16	—	2.9	217	3.0	50,700	169	615	1650	24
me VLD-17	—	38.0	89	2.5	21,200[b]	570	2100	5200	42
me VLD-18	—	—	75	2.3	14,400[b]	570	2020	5030	47
me VLD-19	1.3	—	96	2.0	10,220[b]	180	640	1580	—
me VLD-20	2.6	—	80	2.0	5170[b]	160	610	1650	—
me VLD-21	4.0	—	76	2.0	3240[b]	130	500	1400	—
me VLD-22	4.0	—	74	2.0	3200[b]	160	630	1700	27
me HD-23	—	65	82	2.0	2140	180	590	1500	27
me MD-24	1.1	40	117	3.6	13,570	650	1970	4440	34
me MD-25	0.8	36	91	2.2	20,700	750	2650	6500	44
me MD-26	0.3	22	102	2.7	69,000	920	3300	8400	53
me LLD-27	0.6	32	112	3.2	33,400	920	3100	7500	48

— = not analyzed.
[a] Values of branching parameter g': 0.39 (LD-1), 0.46 (LD-2), 0.19 (LD-3), and 0.22 (LD-4).
[b] At 170°C.

The molecular weight data were measured by SEC at 135°C with a Waters high-temperature instrument 150C (Milford, MA), equipped with three mixed-bed columns (Waters Styragel HT6, HT4, HT3). The columns were calibrated with narrow-MWD polystyrene standards. 1,2,4-Trichlorobenzene was used as a solvent at a flow rate of 1 mL/min. The molecular weight data of the LDPE polymers (LD-1 to LD-4) were reported earlier.[39,40] In that work, we applied the Drott–Mendelson calculation method,[41] which accounts for the influence of LCB with the Zimm–Stockmeyer equation. The reduction in the hydrodynamic volume was measured from the ratio of the intrinsic viscosity of the branched polymer to that of the linear polymer of the same M_w (g', Table I).

The melting curves of the polymers were measured with a PerkinElmer DSC-7 differential scanning calorimeter (Norwalk, CT). The sample weight used was 4–6 mg, and the temperature calibration was performed with Indium (T_m = 156.6°C). For the temperature/area calculation, we used a heat capacity (dH) value of 28.45 J/g for Indium, and for the crystallinity (X_c) determinations, we used the value dH = 290 J/g for 100% crystalline polyethylene. The samples were heated twice from 10 to 160°C at a rate of 10°C/min, and the T_m's and the crystallinities from the second melting are reported in Table I.

The SCs carried out with DSC were performed according to procedures described earlier.[12] By this method, the sample was annealed (120 min at each temperature) in steps at successively lower temperatures. After the annealing steps, we obtained the melting curve of the polymer by heating the cooled sample at a heating rate of 10°C/min up to 150°C, and we analyzed the melting peaks, with the corresponding heights of the separated peaks. Because the melting ranges of the studied polymers varied a lot due to different comonomer content, the crystallization (annealing) temperatures were chosen to observe the highest number and best resolved melting endotherms in the melting curves of each sample.

The DMA measurements were made with a PerkinElmer DMA-7, from compression-molded plaques. The analyses were run at 4°C/min under a helium atmosphere in the temperature scan mode from 135°C up to the T_m of the polymers at a frequency of 1 Hz. The storage modulus (E'), the loss modulus (E''), and the ratio of E'' to E' (tan δ) were recorded.

The rheological measurements were carried out on a Rheometrics Scientific stress-controlled dynamic rheometer (SR-500), equipped with RSI Orchestrator software version 6.4.3 (Piscataway, NJ). The test specimens were compression-molded at 170°C or 190°C for 5 min and allowed to cool under atmospheric pressure. The commercial samples contained antioxidants, and the experimental samples were stabilized with Irganox B215 (Ciba Geigy, Basel, Switzerland) before molding. The measurements were carried out within the linear viscoelasticity region, which was ensured by stress sweeps of each sample. Frequency sweeps for the polymers were carried out under nitrogen at 170°C (VLDPE samples) and 190°C (LLDPE, LDPE, and HDPE samples) with 25-mm plate–plate geometry. The angular frequency ω was varied from 0.02 to 100 rad/s, and the sample gap was 1 mm. For some samples, additional measurements were performed at 150 or 210°C. The Rheometrics RSI Orchestrator software was used to shift the moduli curves along the master curves and to determine the shift factor (a_T). a_T's were then plotted against $1/T$ to obtain the Arrhenius-type flow activation energy (E_a). Only line fits with R-squared values greater than 0.99 were accepted in the line fit.

RESULTS AND DISCUSSION

Melting Behavior

The decrease in crystallinity and the T_m depression with increasing comonomer was more distinct for metallocene-catalyzed copolymers than for ZN copolymers (see Table I). The difference was even more pronounced with higher comonomer amounts. The similarity of the homogeneous V-catalyzed ZNVLD-9 and the metallocene-catalyzed VLDPE polymers was also significant. Figure 1 displays the DSC melting curves obtained after SCs of some of the ZN copolymers and the LDPE-1. The melting endotherms of the copolymers ZNLLD-5, ZNVLD-6, ZNVLD-8, and ZNVLD-10 were characterized by a large endotherm at higher temperatures and several smaller endotherms at lower temperatures. In ZN LLDPE, the highest melting crystals, typically at temperatures above 120°C, were due to the crystallization of polymer chains with higher molecular weights and less comonomer, and the other peaks (typically, six resolved peaks between 85–90 and 117°C) were due to polymer chains with lower molecular weights and higher branching content.[7–9] Only ethylene sequences above a certain critical length between the branches can partici-

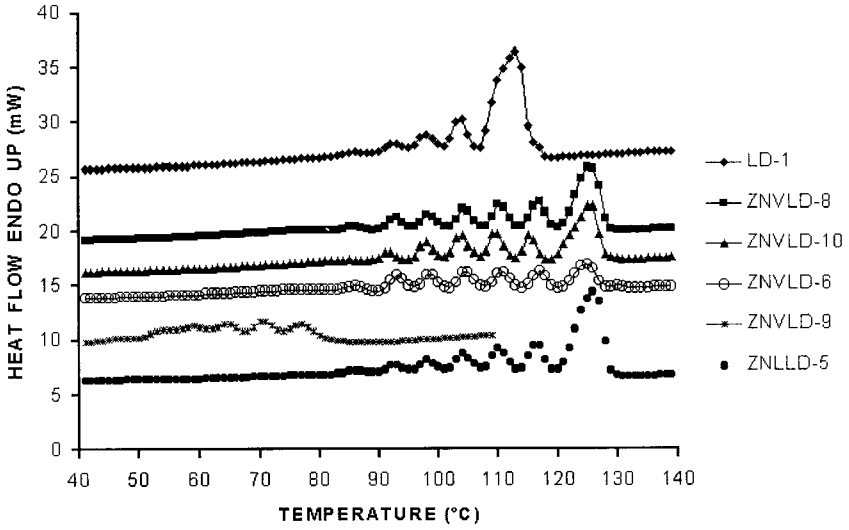

Figure 1 DSC endotherms of ZN copolymers and LDPE sample LD-1 after SC.

pate in the SC process, and a CD is obtained by sorting ethylene segments into thermal fractions or "buckets."[11] The longer segments, recrystallized to larger lamellar crystals, melt at higher temperatures. Ethyl or longer branches are rejected from the crystalline core during the long equilibrium at each isothermal crystallization temperature.[42] The fractionation does not distinguish long branches, but the long branches can participate in the crystallization.[43] Polymer LD-1 displayed an endotherm with only some resolved peaks after the SC. This was due to the narrow SCB of LDPE compared to the ZN copolymers described. The V-catalyzed polymer ZNVLD-9 exhibited an endotherm with six resolved peaks between 45 and 77°C, corresponding to a much narrower CD compared to the ZN copolymers already discussed. This difference was attributed the homogeneous structure of V-based copolymers.[44]

Despite their homogeneous structure, the metallocene copolymers from different processes also showed multiple endotherms at lower temperatures after SC (Fig. 2). A comparison of the endotherm profile of ZNVLD-8 (Fig. 1) with that of meVLD-19 (Fig. 2) illustrates the differences in the CD between ZN and metallocene-catalyzed copolymers of fairly similar comonomer content. A very narrow CD, with no molecules or segments with few branches, could be seen for meVLD-19

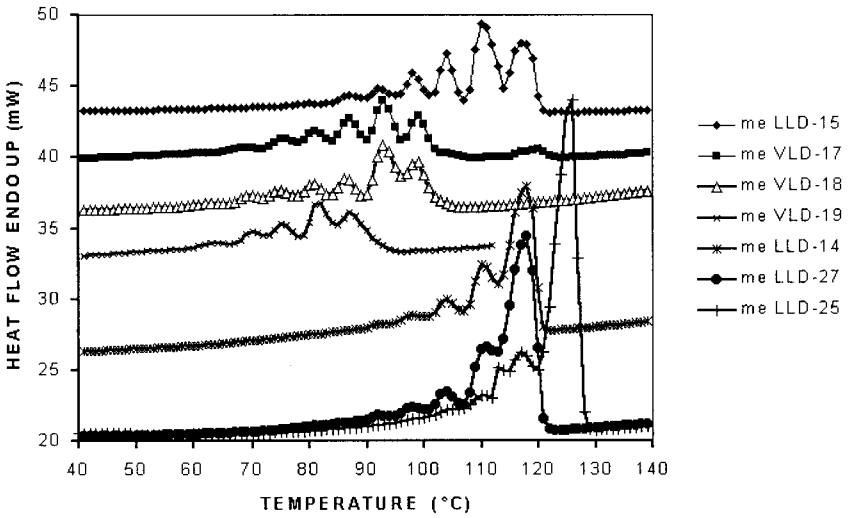

Figure 2 DSC endotherms of metallocene-catalyzed copolymers after SC.

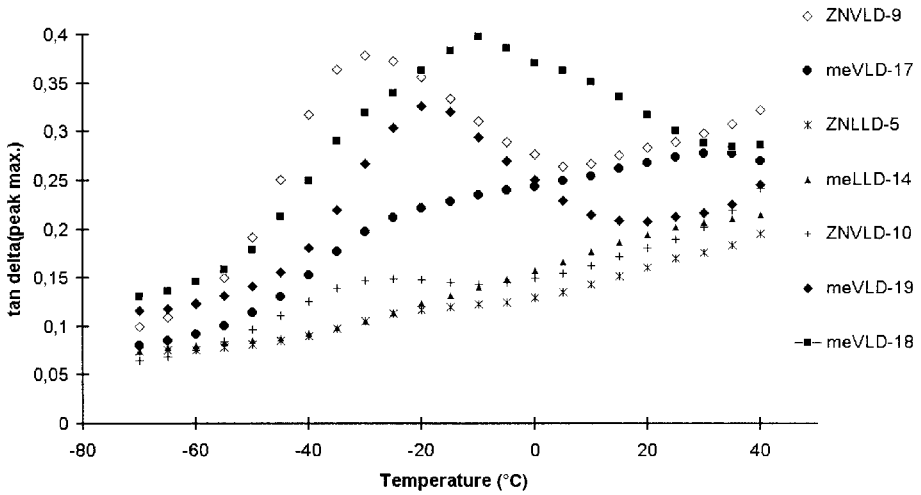

Figure 3 DMA curves (tan δ) of ZN- and metallocene-catalyzed copolymers.

(separated segregated peaks between 64 and 88°C), meVLD-17, and the CGC-catalyzed meVLD-18. Slightly broader distributions existed for the metallocene-catalyzed LLDPE and MDPE copolymers meLLD-15 (peaks from 79 to 118°C), meLLD-14 (peaks from 92 to 118°C), and meMD-25 (peaks from 104 to 125.5°C). The endotherm of meVLD-17 displayed a main melting range from about 70 to 100°C, but interestingly, there were traces of additional melting from 115 to 120°C, which suggests that this polymer might have been a blend containing a minor amount of ZN LLDPE or possibly LDPE. Our experimental polymer meLLD-27 exhibited a nearly identical pattern of peaks to the commercial-grade meLLD-14, indicating similar short-chain branching distribution (SCBD). The behavior of metallocene-catalyzed VLD polymers 21 and 22 (not shown in Fig. 2 for clarity) indicated a similar narrow distribution of branches to polymer meVLD-19. The results demonstrate that metallocene copolymers displaying similar M_w's and MWDs may exhibit different SCBDs due to the different catalysts and polymerization processes, but the most typical feature is their narrow SCBD compared to the ZN copolymers.

Qualitative conclusions regarding the morphology have been drawn with the Gibbs–Thomson equation for relating the T_m's and the lamellar thicknesses of linear polyethylenes and ethylene copolymers.[11,45] However, its use for copolymers has been questioned.[42] A more detailed discussion of the differences in lamellar thicknesses of ZN and metallocene-catalyzed copolymers is given in a recent report.[46]

Dynamic Mechanical Behavior

β relaxations, which are most sensitive to the effect of branching, can be studied from E'' and tan δ curves in DMA analysis. From the curves, the temperatures for the β relaxations were noted and the values for the maximum tan δ value, corresponding peak temperature (T), and the temperature for $E''_{(max)}$ were calculated (Table I). Figure 3 displays a comparison of the tan δ curves of some of the ZN- and metallocene-catalyzed copolymers. In accordance with earlier results,[19] there was only a slight increase in the intensities of the tan δ maximum peaks of heterogeneous copolymers with the incorporation of more comonomer (more branching). However, the V-catalyzed copolymer ZNVLD-9 displayed a very intense tan δ peak. This significant increase in intensity of the β transition, reported earlier by Clas et. al.,[47] was due to the increasing amorphous content as the branch concentration grew. The metallocene copolymers also exhibited strong transitions in the tan δ curves at greater comonomer content, which was an indication of the high comonomer response of these catalysts. Polymer meVLD-18, produced with a CGC catalyst, displayed the highest intensity value of the curves, as shown in Figure 3. We suggest that this spectral narrowing of the tan δ peak of the metallocene copolymers compared to the ZN copolymers was an indication that the local environment near the branch point, which gave rise to the amorphous phase, was becoming more homogeneous.[17,18] For more branched copolymers (VLDPEs), the location and the size of the β relaxation peak dis-

played the differences in SCBDs between metallocene and ZN copolymers.[17] The differences in the CDs for our copolymers found by SC by DSC were supported by the DMA results.

Polymer meVLD-17 exhibited a tan δ curve that differed from those of pure metallocene and heterogeneous polymers. The higher intensity values at higher temperatures indicate the presence of a heterogeneity already revealed from the melting behavior (Fig. 2). For studies of the effect of small differences in comonomer or branching amounts, the $E''_{(max)}$ temperatures seemed to give the best information. A decrease in $E''_{(max)}$ temperature with increasing comonomer content could be confirmed for meVLD-19, meVLD-20, and meVLD-21, all synthesized in the same process. In accordance with results by Keating and Lee,[48] we also found that the location of the β transitions of the metallocene-catalyzed ethylene–butene copolymers appeared at higher temperatures than for ZN ethylene–butene copolymers of equivalent compositions, despite the lower crystallinity values of the metallocene copolymers. The tan δ intensity of the metallocene materials was higher (meVLD-21 vs. ZNVLD-6 and meVLD-19 vs. ZNVLD-8, as shown in Table I). We suggest that this difference is related to the ability of the metallocene copolymers to have a higher degree of subambient crystallization due to a larger population of ethylene segments below the critical ambient crystallization lengths.[48]

Rheological Properties

Rheological behavior of the polymer melts was studied with dynamic rheological measurements. The complex viscosity (η^*) from dynamic measurements, calculated as

$$\eta^* = ((G'/\omega)^2 + (G''/\omega)^2)^{1/2} \quad (1)$$

where G' represents the elastic component (storage modulus) and G'' the viscous component (loss modulus) of the melt response as a function of radian frequency (ω), was approximately equal to the steady η, when compared at equal frequency and shear rate. To compare viscosity data with M_w and M_w/M_n data, we used the η^*'s taken at 0.02 rad/s [given in Table II as η^* (0.02 rad/s)]. As discussed by Carella,[28] these values cannot be taken as real values of the zero shear viscosity (η_0), but they are still useful for the evaluation of properties. For comparison of the elasticity levels, we applied the method of Han,[49] according to which the elasticity can be evaluated by plotting G' versus G''. Shroff and Mavridis[50] evaluated the value of G' at a fixed low value of G'' to gain a measure of M_w/M_n at the high-molecular-weight end of the MWD. This value, called E_R, is independent of M_w and temperature of measurement but is influenced by MWD and LCB. This method of quantifying the effects of MWD and LCB in polyolefins has recently also been applied to metallocene polyethylenes,[51,52] giving partly contradictory results about the influence of MWD. Throughout our work, we have accepted the definition that G' represents the elastic component of the viscoelastic melt and is, therefore, associated with the melt elasticity, although Khanna and Slusarz[53] pointed out that certain cautions should be exercised when relating G' to the melt elasticity in the processing of a polymer. In this work, we compared the G' values at three different values of G'': 2000, 5000, and 10,000 Pa (values in Table II).

HDPE Polymers

Figure 4 presents the η^*'s at 190°C versus the radian frequencies of the heterogeneous and homogeneous HDPE polymers. A comparison of the heterogeneous polymers ZNHD-11, ZNHD-12, and ZNHD-13 reveals remarkable differences in the η^* (0.02 rad/s) values, which can be correlated to the M_w data but not to the M_w/M_n values given in Table II. A rather similar shear-thinning behavior was characteristic for these samples. The Cr-catalyzed ZNHD-12 exhibited the highest elasticity G' at reference value of $G'' = 10^4$ Pa, which was most probably related to its significant high-molecular-weight part, typical for polyethylenes synthesized with this type of catalyst.

The curves of the two homogeneous metallocene-catalyzed polyethylenes meHD-16 and meHD-23 exhibited very little shear-thinning behavior, a drawback typical for the narrow-MWD metallocene-catalyzed polyethylenes. The big difference in the M_w explains the much higher viscosities of meHD-16, and its elasticity level (G' values in Table II) was also slightly higher. Despite the relatively similar and narrow MWD values, the metallocene-catalyzed polymer meMD-26 exhibited quite a different flow behavior compared to the metallocene-catalyzed polymers meHD-16 and meHD-23. Indeed, polymer meMD-26 exhibited flow behavior very similar to that of ZNHD-13, despite the big differences in their molecular weight data (the SEC-measured M_w for meMD-26

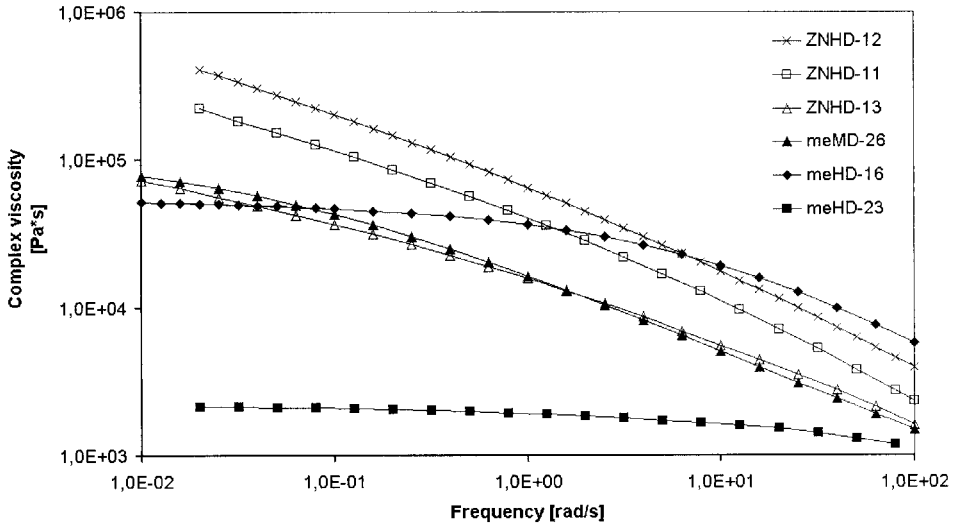

Figure 4 η^* vs. ω of ZN- and metallocene-catalyzed HDPEs measured at 190°C.

was 102,000 g/mol and MWD = 2.7, whereas ZNHD-13 gave M_w = 240,000 g/mol and MWD = 23.3). The elasticity values of meMD-26 were higher than those of ZNHD-13 at G'' 5000 and 10000 Pa, although the M_w of meMD-26 was much lower and the MWD was much narrower than those of ZNHD-13. The high-flow E_a value of the meMD-26 in Table II suggests that this behavior may indicate the presence of LCB, and this is discussed in more detail later.

LLDPE Polymers

A comparison of heterogeneous and homogeneous LLDPE copolymers is given in Figure 5. The heterogeneous copolymer ZNLLD-5 displayed well-known shear-thinning behavior. On the contrary, the two homogeneous metallocene-catalyzed copolymers meLLD-14 and meLLD-15 exhibited viscosity curves that were almost totally independent of the frequency, which means that the processing of these polymers may raise difficulties. Again, one of the metallocene samples, polymer meLLD-27 (which in the DSC measurements displayed a very similar CD to me-LLD14), displayed stronger shear-thinning behavior and higher elasticity values (G' values in Table II) than the other metallocene-catalyzed LLD polymers. This behavior was still more pronounced for

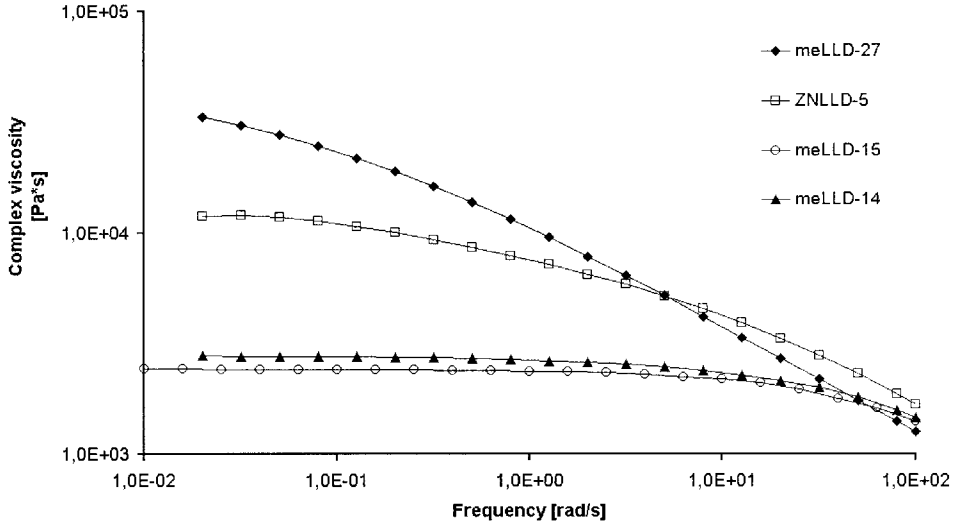

Figure 5 η^* vs. ω of heterogeneous and homogeneous LLDPEs measured at 190°C.

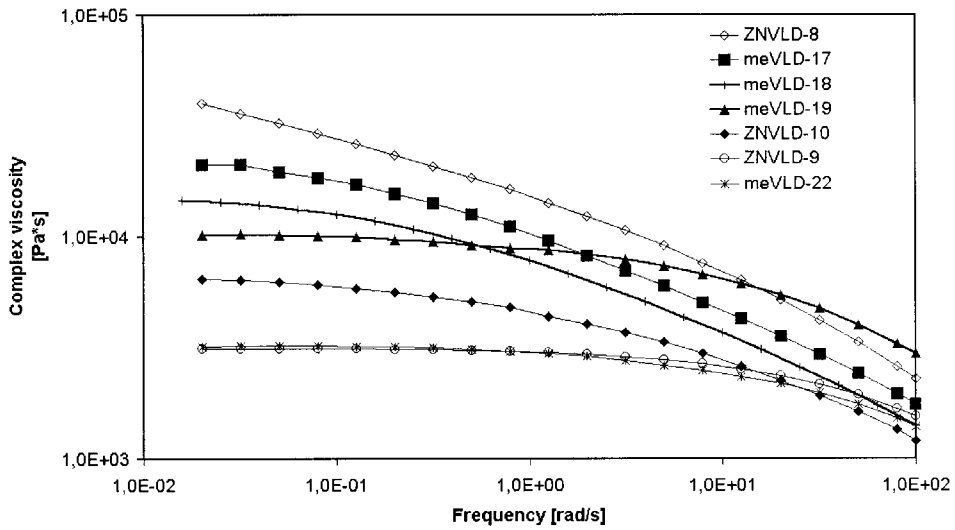

Figure 6 η^* vs. ω of heterogeneous and homogeneous VLDPEs measured at 170°C.

meMD-26 (not shown in Fig. 5, values in Table II). This combination of strong shear thinning and higher elasticity values make this type of polymer very interesting from the processing point of view.

VLDPE Polymers

Figure 6 displays the frequency dependence of three heterogeneous VLDPE copolymers made by different processes and four metallocene-catalyzed VLDPE copolymers. The heterogeneous copolymers all showed shear-thinning behavior, but for polymer ZNVLD-10, the shear thinning was less pronounced than for polymer ZNVLD-8. The low MFR polymer ZNVLD-8, which displayed the highest M_w, also exhibited the highest η^* throughout the whole measured frequency range. The two linear metallocene-catalyzed copolymers, meVLD-19 and meVLD-22, both exhibited highly frequency-independent behavior (long Newtonian plateau), and the same behavior was also seen in the curves (not displayed in the figure) of polymers meVLD-20 and meVLD-21 produced under very similar process conditions. For this specific group of copolymers the η^* (0.02) values and the viscosity curves were in accordance with the MFR and the M_w values given. The frequency curve of the homogeneous V-catalyzed ZNVLD-9 was interestingly identical to that of the metallocene-catalyzed meVLD-22. The M_w, MWD, MFR, and density values and the butene contents of these two polymers were very close, but they were produced in different processes and with different catalyst systems. This limiting behavior and the presence of a Newtonian plateau at low frequencies was mentioned for VLDPEs commercialized by Mitsui.[54] Our comparison thus seems to confirm that polymers of closely identical rheological properties can be produced both with V and metallocene catalysts. The flow curves of the metallocene-catalyzed polymers meVLD-17 and meVLD-18 displayed a different shear-thinning behavior compared to the other (non-LCB) metallocene-catalyzed copolymers, as shown in Figure 6. We relate this difference to long-chain branches in meVLD-17 and meVLD-18.

Temperature Dependence

The temperature dependence of viscosity is one of the most important variables in polymer flow, and this dependency can be expressed by an Arrhenius-type equation

$$\eta = Ae^{(E_a)/RT} \tag{2}$$

where η is the viscosity, R is the gas constant, A is the constant, T is the temperature, and E_a is the flow activation energy.[55] E_a varies widely from polymer to polymer and depends on chain composition. A higher E_a indicates greater viscosity reduction with increasing temperature. The E_a's of HDPE flow curves, according to Ariavan et al.,[56] normally lie in the range from 20 kJ/mol to 28 kJ/mol. In their study on HDPE blow-molding resins, Ariawan et al.[56] found no apparent correlation between molecular parameters and the E_a

for resins with a narrow MWD. For M_w/M_n's greater than 10, however, the concentration of large molecules became important, and increasing the concentration increased the E_a. The effect of branching on the E_a of polyethylenes has been found to be even more significant[27,30,55,57–59] than the M_w/M_n. Hughes[57] and Bersted[58] analyzed the effect of a very low degree of LCB on the flow E_a and explained that such small amounts of LCB can be determined from an increase in E_a. Small amounts of LCB were found to have a very large effect on the rheological properties of HDPE melts at low frequencies but not at high frequencies. Recent reports by Wasserman and Graessley[60] and Shroff and Mavridis[51] discuss the influence of different molecular parameters on the flow E_a's of polyolefins. It has been proposed that the flow E_a of LLDPE with octene as a comonomer is higher than that of an LLDPE with butene as a comonomer.[55] Vega and coworkers[30,52] found a correlation between the E_a of the flow of copolymers of ethylene and hexene and the degree of hexyl branching. According to this correlation, an E_a of about 34 kJ/mol was obtained for copolymers having a degree of butyl branching of 20 per 1000 carbon atoms. They obtained values of 29–38 kJ/mol for the flow E_a's of metallocene HDPEs, which according to Carella,[28] must be an indication of the presence of LCB. A recent article by Vega et al.[52] suggests that metallocene polymers, with reference to their M_w and MWD, show abnormal rheological behavior and some higher flow E_a values and may posses low amounts of LCB. This is in accordance with the values 32–40 and 40–45 kJ/mol for CGC-catalyzed ethylene–octene copolymers, as reported by Kim et al.[25] and by Hatzikiriakos et al.,[61] respectively, where the CGC polymers contained LCB.

The results in Table II display E_a values of 25 kJ/mol for both ZNHD-12 and meHD-16. This is in accordance with literature numbers[28,52,53,55,56] for linear polyethylenes and seems to confirm that the high elasticity values obtained for ZNHD-12 were due to the high-molecular-weight tail and not to any noticeable amount of longer branches. Also, our experimental homogeneous polymer meHD-23 displayed a very low E_a value, according to our expectations. Our LDPE polymers all showed high E_a values within the range reported in the literature (48–67 kJ/mol). Surprisingly, we obtained a higher value for the low-M_w, narrow-MWD polymer LD-2 than for the high-M_w, broad-MWD polymer LD-3. This might be explained by the fact that the broad MWD of polymer LD-3 may have been a result of the high-molecular-weight species shown in the tail of the MWD curve of the polymer and not due to a higher amount of branching. Such behavior has been suggested by Mirabella and Wild[62] for this type of polymer.

Our own experimental metallocene-catalyzed polymers 24–27, as well as the commercial meVLD-17, meVLD-18, and meVLD-26, displayed flow E_a values in a much higher range than is typical for linear polyethylenes. These high E_a values, together with the rheological behavior (significantly high low-η with reference to M_w and MWD), confirm our findings that we have to deal with metallocene-catalyzed polymers that contain LCB. However, polymer meVLD-17, according to the DSC and DMA results, contained partly heterogeneous material, and we were unable to separate the effect of this component on the activity energy.

Wang et al.[34] emphasized that the ratio of MFR at 10 kg load (MFR_{10}) to that at 2.16 kg load (MFR_2) can be increased, at almost constant M_w/M_n, by increasing the LCB frequency. This high sensitivity of MFR_{10}/MFR_2 to LCB made the MFR_{10}/MFR_2 a good rheological measurement for LCB in their studies. A comparison of the flow E_a values with the MFR_{21}/MFR_2 values in Table II for the metallocene-catalyzed polymers 24–27 seemed to support these findings. The increasing E_a ($34 < 44 < 48 < 53$ kJ/mol) of meMD-24, meMD-25, meLLD-27, and meMD-26 was followed by increasing ratios of MFR_{21}/MFR_2 ($36.3 < 45 < 53.3 < 73$). Although the M_w/M_n's were not quite constant for the polymers listed, we conclude that an increase in branching was followed by increases in MFR_{21}/MFR_2.

Elasticity and LCB

The influence of the molecular composition, which controls the relaxation times at long times, is also revealed in G' and G'' at low frequencies.[63] According to earlier results by Furumiya et al.,[64] the frequency-dependence curves of ZN LLDPE melts are clearly different from those of LDPE in their shapes: Both G' and G'' curves for LLDPE are much steeper than those for LDPE, which indicates that the distribution of relaxation times is broader in LDPE than in ZN LLDPE. On account of the similarity in MWD of their studied samples, the differences in curve shapes were related to branching effects rather than MWD. Earlier results by Utracki and Schlund[65] demonstrated that the melt elasticity of ZN LLDPE, as mea-

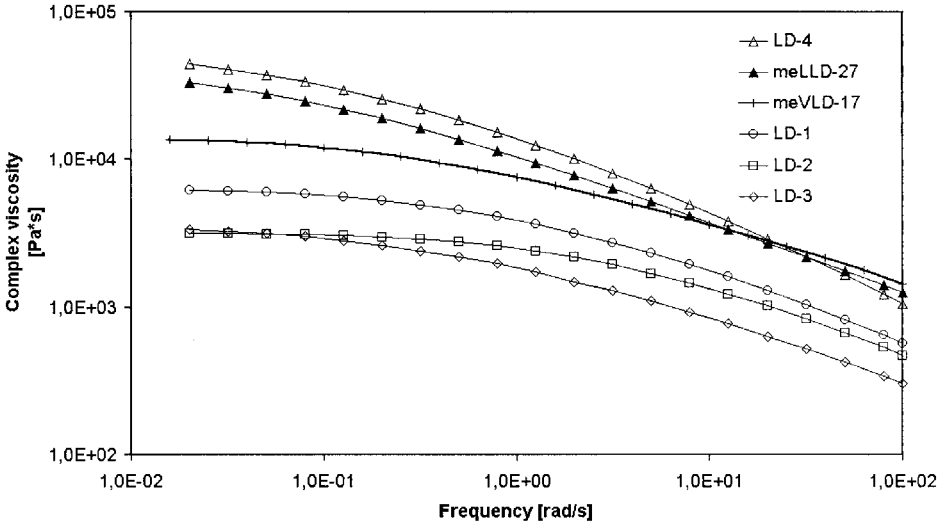

Figure 7 η^* vs. ω of long-chain branched polyethylenes measured at 190°C.

sured by G', is independent of the SCB level. Dormier et al.,[66] in their studies on the influence of M_w and MWD on differences in the low-frequency behavior of ZN LLDPEs, demonstrated that the high-molecular-weight components increased the G' values in the low-frequency area. Early findings by Wild et al.[67] concluded that G' of LDPE at low frequencies was clearly higher for the more branched samples, although the frequency dependence of η^* was very similar. According to findings on the structures of LLDPE and HDPE by Wong et al.,[68] log G' versus log G'' was strongly dependent on MWD but also on molecular structures such as long-chain branches. Lachtermacher and Rudin[69] found, in their studies on peroxide treated LLDPE, that the increased relative contribution of the G' response to that of G'' may also be a result of an increased degree of LCB. The dramatic effect of small amounts of LCB on the rheological properties of linear polymers has been extensively reviewed by Shroff and Mavridis.[50]

Figure 7 shows the η^* curves of the analyzed LDPE polymers LD-1 to LD-4 with varying LCB content, the polymer meVLD-17, and one of our experimental LCB polymers, meLLD-27. Bear in mind that although resins with the same manufacturing technology (LD-2, LD-3, and LD-4) were studied, the amount and distribution of branching may have been altered by the change in process conditions along with the amount of initiators and chain-transfer agents in the high-pressure process. The difference in the broadness of MWD between LD-2 and LD-3 was clearly seen in the higher shear-thinning behavior of the high-M_w polymer LD-3. Despite the different M_w's and MWDs, the level of η^* at low shear rates and the shear sensitivities of LD-4 and meLLD-27 were very similar. Moreover, meLLD-27 yielded flow E_a in the range of the LDPEs. By plotting the G' as a function of the G'' in Figure 8, we illustrate the contribution of the elastic component and the viscoelastic component in the viscoelasticity of resins LD-1, LD-2, LD-3, and meLLD-27. The effect of the M_w and MWD on the elasticity at low shear rates is demonstrated for the LDPEs. The difference in the behavior of the narrow MWD, low M_w, and according to SEC analyses, slightly branched polymer LD-2 and the broad MWD, high M_w, and highly branched polymer LD-3 was significant. The differences in G' values at lower frequency (Table II) were in accordance with the influence of the LCB found by Wild et al.,[66] although we were not able to fully separate the effect of MWD and branching. We did not notice any M_w or MWD effect on the elasticity numbers of the ZN-catalyzed LLDPE and VLDPE copolymers, but this may be have been due to different processes used in the manufacturing of these resins. The curve of meLLD-27 partly overlayed the curve of the highly branched LD-4 (about the same MFR values, not shown in the figure for clarity), which supports our earlier conclusion about the presence of LCB in this sample. For the nonbranched HDPE polymers ZNHD-11, ZNHD-12, and ZNHD-13, we could not confirm any MWD effect on the elasticity values in Table II. However, a higher M_w, often a result of a high molec-

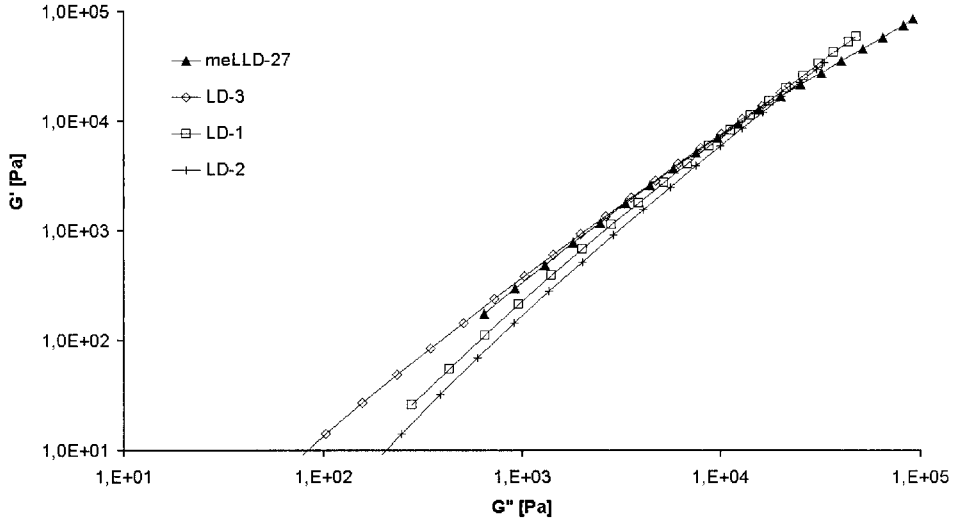

Figure 8 G' versus G'' of long-chain branched polyethylenes measured at190°C.

ular tail in Cr-catalyzed polyethylenes, seemed to result in higher G' numbers in ZNHD-12.

To further confirm the differences in elasticity between our experimental copolymers, we displayed the G' as a function of the G'' in Figure 9. Despite their similar MWDs, the curves of the copolymers meLLD-27, meVLD-17, and meVLD-18 were quite different from those of the homogeneous V-catalyzed ZNVLD-9 and the homogeneous linear meVLD-20. These differences were also seen in the G' numbers, as shown in Table II. Polymer meVLD-18 was synthesized with a CGC catalyst, and this type of polymer, according to recent reports already mentioned, contains LCB. This was also supported by the value of the flow E_a (47 kJ/mol, given in Table II). The high activity energy values of meVLD-17 (42 kJ/mol) and meLLD-27 (48 kJ/mol) and the shapes of the G' versus G'' curves, including the CGC-catalyzed meVLD-18 in Figure 9, most probably resulted from the presence of LCB in these polymers. The G' numbers in Table II also display the similarity in elastic behavior of meLLD-27 and meMD-26. We believe that careful determination of the relationships between G' and G'' is a valuable tool when studying elasticity and LCB in polyethylenes, together with reliable MWD and M_w data from SEC analyses.

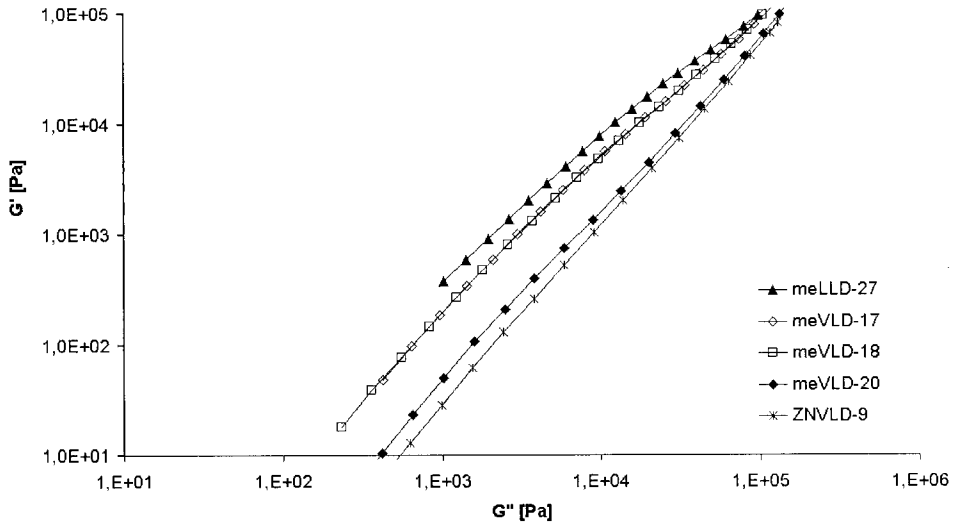

Figure 9 G' versus G'' of homogeneous copolymers measured at 170°C.

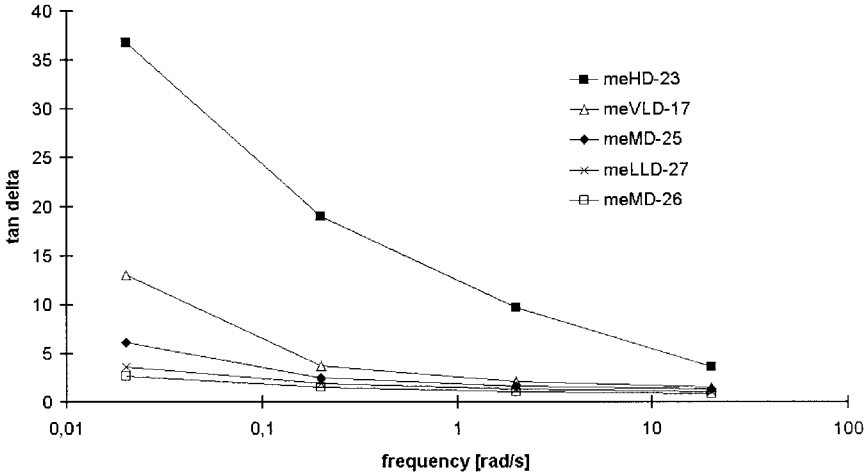

Figure 10 Tan δ versus ω of metallocene polymers measured at 190°C.

Some authors[70–72] have plotted tan δ (G''/G') versus frequency from small-amplitude oscillatory shear in their studies of the viscoelasticity of polyolefins. Booij[70] suggested that the phase angle δ versus angular frequency yields information about LCB and viscoelasticity of ethylene–propylene–diene elastomers. Chambon[71] used the tan δ–frequency relationship by ranking PP material; the flatter the tan δ trace was, the broader MWD and the steeper the tan δ was, the narrower MWD was. Haxlitt et al.[72] measured the frequency dependency from rheological measurements to explain the elasticity of polymers (related to the M_w/M_n or MWD). They found, for their LLDPE samples (most probably of ZN type because the MWDs were 3.3–6.2), that lower tan δ values at low frequencies and broader MWDs were characteristic of a polymer that relaxes slowly (longer relaxation times). It is known[70] that highly extended structures of branched polymer molecules show exceptionally long relaxation times. We, therefore, suggested that a low slope in the lower frequency range of the tan δ versus frequency corresponds to a more elastic melt for a given polymer. To check the usefulness of the tan δ concept, we applied the method to our experimental metallocene-catalyzed grades and the homogeneous copolymer meVLD-17 (Fig. 10) at 190°C. Only small differences in MWDs existed for these polymers, but the flow E_a values, as shown in Table II, exhibited significant variations. The results of meHD-23 were not readily comparable with the others due to the different viscosity level of meHD-23. Nevertheless, the slope of the tan δ curves, as shown in Figure 10, decreased with increasing E_a values: 27 kJ/mol ("linear" meHD-23), 42 kJ/mol (meVLD-17), 44 kJ/mol (meMD-25), 48 kJ/mol (meLLD-27), and 53 kJ/mol (meMD-26). Shroff and Mavridis[51] recently discussed the thermorheological complexity in the determination of E_a with data on LLDPE modified with peroxide. They found a clear lack of superposition at low frequencies in the plot of tan δ versus frequency and made the conclusion that the computation of E_a depends highly on the frequency range of data. Despite these uncertainties, we believe that an analysis of the curvature of the loss tangent trace can deliver information about the branching levels, at least for polymer families synthesized in similar processes. However, much of the same information lies in the G' curves.

It is well known that correlations between Newtonian viscosity and M_w can be established. Relationships between η_0 and M_w have been reported, and an often-used equation was proposed by Raju and coworkers[73] for linear polyethylene fractions at 190°C:

$$\eta_0 = 3.4 \times 10^{-15}(M_w)^{3.6} \tag{3}$$

The solid line in Figure 11 represents this equation. Figure 11 presents dynamic viscosity data at 190°C, taken at a frequency 0.02 rad/s (not identical to η_0) as a function of the M_w of several ZN- and metallocene-catalyzed polymers. The low-frequency η^* of the ZN-catalyzed and the linear metallocene copolymers approximately followed the 3.6 dependence of M_w, but our suspected long-chain branched polymers deviated upward from the line. Considering the rather low molecular

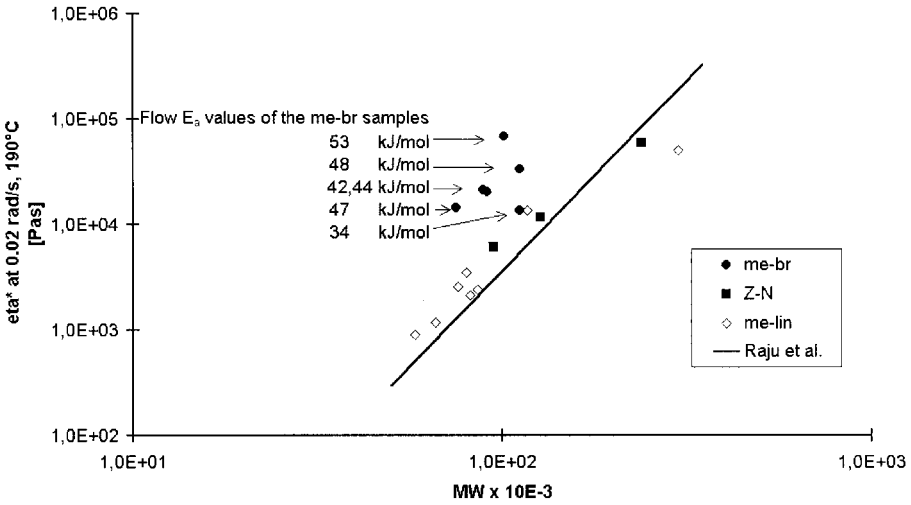

Figure 11 Correlation of M_w and η^* at 0.02 rad/s and 190°C: (■) ZN-catalyzed polymers, (◇) linear metallocene-catalyzed polymers, and (●) suspected long-chain branched metallocene polymers.

weight data of these polymers, given in Table II, we did not expect the presence of an extremely high-molecular-weight linear species in the polymers to cause the high η^*'s but rather the presence of long-chain branches. A common feature for the polymers shown in Figure 11, which gave higher viscosities, was also their higher flow activation values (meVLD-17, meVLD-18, meMD-25, meMD-26, and meLLD-27). These findings are in agreement with results presented by Vega et al.[30] and Malmberg et al.[37] and support the proposal[30] that viscosity–M_w plots can distinguish between long-chain branched and non-long-chain branched polyethylenes.

CONCLUSIONS

We evaluated the thermodynamic and melt rheological properties of PE homopolymers and copolymers synthesized with different catalysts and in different polymerization processes. The comonomer composition distribution was analyzed with SC by DSC and DMA. The heterogeneous ZN copolymers were characterized by much broader comonomer and lamellar thickness distributions than the metallocene copolymers. The V-catalyzed VLDPE displayed similar effective comonomer incorporation to the metallocene copolymers at the same density level.

The melt flow curves of our studied Ziegler–Natta high-density polyethylene (ZN HDPE) resins exhibited significant differences in the η^* (0.02 rad/s) values, which were found to depend on M_w and MWD. The elasticity values (G') increased with increasing M_w. Homogeneous metallocene HDPE resins exhibited very little shear-thinning behavior, in accordance with their narrow-MWD and linear (non-LCB) structure. The expected trend of increasing viscosity with M_w and shear-thinning tendency with M_w/M_n was observed for the heterogeneous LLDPE and VLDPE resins and for the narrow-MWD, linear metallocene LLDPE and VLDPE resins. With regard to the flow E_a, the heterogeneous ZN HDPE polymers exhibited values close to 25 kJ/mol, and the LDPE polymers exhibited values in the range of 50–60 kJ/mol, in accordance with literature data. Some of the metallocene-catalyzed commercial and experimental resins exhibited E_a values between 34 and 53 kJ/mol, which indicate LCB. The long-chain branched metallocene copolymers displayed higher low-shear viscosities and earlier onset of shear thinning than the non-LCB copolymers of similar molecular weight. In addition, an increasing E_a was followed by an increasing MFR_{21}/MFR_2, markedly increased value of G', and smaller slopes when tan δ was expressed as a function of frequency.

REFERENCES

1. Sinn, H.; Kaminsky, W. Adv Organomet Chem 1980, 18, 99.

2. Knight, G. W.; Lai, S. Proc Soc Plast Eng RETEC 1993, 2, 226.
3. Foster, G. H.; Wasserman, S. H. MetCon97: Polymers in Transition, June 4–5, 1997, Houston, TX; The Catalyst Group: Springhouse, PA.
4. Todo, A.; Kashiwa, W. Macromol Symp 1996, 101, 301.
5. Wild, L. Adv Polym Sci 1990, 98, 1.
6. Xu, J.; Xu, X.; Feng, L. Eur Polym J 1999, 36, 685.
7. Kamiya, T.; Ishikawa, T.; Kambe, S.; Ikeyami, N.; Nischibu, H.; Hattori, T. Soc Plast Eng Tech Pap Annu Tech Conf 1990, 36, 871.
8. Adisson, E.; Ribeiro, M.; Deffieux, A.; Fontanille, M. Polymer 1992, 33, 4339.
9. Balbontin, G.; Camurati, I.; Dall'Occo, T.; Finotti, A.; Franzese, R.; Vecellio, D. Angew Makromol Chem 1994, 219, 139.
10. Keating, M.; McCord, E. F. Thermochim Acta 1994, 243, 129.
11. Minick, J.; Moet, J.; Hiltner, A.; Baer, A.; Chum, S. P. J Appl Polym Sci 1995, 58, 1371.
12. Starck, P. Polym Int 1996, 40, 111.
13. Keating, M.; Lee, I.-H.; Wong, C. S. Thermochim Acta 1996, 284, 47.
14. Mueller, A. J.; Hernandez, Z. H.; Arnal, M. L.; Sanchez, J. J. Polymer Bull 1997, 39, 465.
15. Shanks, R. A.; Drummond, K. M. Proc Soc Plast Eng Tech Pap Annu Tech Conf 1998, 44, 2004.
16. Khanna, Y. P.; Turi, E. A.; Taylor, T. J.; Vickroy, V. V.; Abbot, R. F. Macromolecules 1985, 18, 1302.
17. Woo, L.; Ling, M. T. K.; Westphal, S. P. Thermochim Acta 1994, 243, 147.
18. Westphal, S. P.; Woo, L.; Ling, T. K. Thermochim Acta 1996, 272, 181.
19. Starck, P. Eur Polym J 1997, 33, 339.
20. Bensason, S.; Minick, J.; Moet, A.; Chum, S.; Hiltner, A.; Baer, A. J Polym Sci Part B: Polym Phys 1996, 34, 1301.
21. Kalyon, D. M.; Yu, D.-W.; Moy, F. H. Polym Eng Sci 1988, 28, 1542.
22. Mendelson, R. A.; Bowles, W. A.; Finger, F. L. J Polym Sci A 1970, 2(8), 105.
23. Wild, L.; Ranganath, R.; Ryle, T. J Polym Sci 1971, 9, 2137.
24. Lai, S.; Plumley, T. A.; Butler, T. A.; Knight, G. W.; Kao, C. I. Soc Plast Eng Tech Pap Annu Tech Conf 1994, 40, 1814.
25. Kim, Y. S.; Chung, C. I.; Lai, S. Y.; Hyan, K. S. J Appl Polym Sci 1996, 59, 125.
26. Hamielec, A.; Soares, J. B. P. Prog Polym Sci 1996, 21, 651.
27. Vega, J. F.; Muñoz-Escalona, A.; Santamaria, A.; Muñoz, M. E.; Lafuente, P. Macromolecules 1996, 29, 960.
28. Carella, J. M. Macromolecules 1996, 29, 8280.
29. Muñoz-Escalona, A.; Lafuente, P.; Vega, J. F.; Muñoz, M. E.; Santamaria, A. Polymer 1997, 38, 3.
30. Vega, J. F.; Santamaria, A.; Muñoz-Escalona, A.; Lafuente, P. Macromolecules 1998, 31, 3639.
31. Zhu, S.; Li, D. Macromol Theory Simul 1997, 6, 797.
32. Malmberg, A.; Kokko, E.; Lehmus, P.; Löfgren, B.; Seppälä, J. V. Macromolecules 1998, 31, 8448.
33. Schellenberg, J.; Schutz, U. Angew Macromol Chem 1998, 255, 5.
34. Wang, W.-J.; Yan, D.; Charpentier, P. A.; Zhu, S.; Hamielec, A. Macromol Chem Phys 1998, 199, 2409.
35. Bin Wadud, S. E.; Baird, D. G. Soc Plast Eng Tech Pap Annu Tech Conf 1999, 45, 1200.
36. Wood-Adams, P.; Dealy, J. M. Soc Plast Eng Technical Papers Annu Tech Conf 1999, 45, 1205.
37. Malmberg, A.; Liimatta, J.; Lehtinen, A.; Löfgren, B. Macromolecules 1999, 32, 6687.
38. Kokko, E.; Malmberg, A.; Lehmus, P.; Löfgren, B.; Seppälä, J. V. J Polym Sci Part A: Polym Chem 2000, 38, 376.
39. Kulin, L. I.; Meijerink, N. J.; Starck, P. Pure Appl Chem 1988, 60, 1403.
40. Starck, P. Helsinki University of Technology, unpublished results.
41. Drott, E. E.; Mendelson, R. A. J Polym Sci Polym Chem Ed 1970, 8, 1361.
42. Lu, L.; Alamo, R. G.; Mandelkern, L. Macromolecules 1994, 27, 6571.
43. Alamo, R. G.; Mandelkern, L. Thermochim Acta 1994, 238, 155.
44. Hunter, B.; Russel, K. E.; Scammel, M. V.; Thomson, S. L. J Polym Sci Polym Chem Ed 1984, 22, 1383.
45. Hosoda, S. Polym J 1988, 20, 5, 383.
46. Jokela, K.; Starck, P.; Väänänen, A.; Torkkeli, M.; Serimaa, R.; Löfgren, B.; Seppälä, J. V. J Polym Sci Part B: Polym Phys 2000, 39, 1860.
47. Clas, S.-D.; McFaddin, D. C.; Russell, K. E. J Polym Sci Part B: Polym Phys 1987, 25, 1057.
48. Keating, M. Y.; Lee, I. J Macromol Sci Phys 1999, 38, 379.
49. Han, C. D. J Appl Polym Sci 1988, 35, 167.
50. Shroff, R.; Mavridis, H. J Appl Polym Sci 1995, 57, 1605.
51. Shroff, R.; Mavridis, H. Macromolecules 1999, 32, 8454.
52. Vega, J. F.; Fernandez, M.; Santamaria, A.; Muñoz-Escalona, A.; Lafuente, P. Macromol Chem Phys 1999, 200, 2257.
53. Khanna, Y. P.; Slusarz, K. R. Polym Eng Sci 1993, 33, 122.
54. Kim, B. Y.; Kim, M. S.; Jeong, H. M.; King, K. J.; Jang, J. K. Angew Macromol Chem 1992, 194, 9.
55. Wang, J. S.; Porter, R. S. Rheol Acta 1995, 34, 496.
56. Ariawan, A. B.; Hatzikiriakos, S. G.; Hay, H.; Goyal, S. K. Soc Plast Eng Tech Pap Annu Tech Conf 1999, 45, 1005.
57. Hughes, J. K. Soc Plast Eng Tech Pap Annu Tech Conf 1983, 29, 306.
58. Bersted, B. H. J Appl Polym Sci 1985, 30, 3751.

59. Mavridis, H.; Shroff, R. N. Polym Eng Sci 1992, 32, 1778.
60. Wasserman, S. H.; Graessley, W. W. Polym Eng Sci 1996, 36, 852.
61. Hatzikiriakos, S. G.; Kazatchkov, I. B.; Vlassopoulos, D. J Rheol 1997, 41, 1299.
62. Mirabella, F.; Wild, L. Polym Mat Sci Eng 1988, 59, 7.
63. Fleissner, M. Makromol Chem Macromol Symp 1992, 61, 324.
64. Furumiya, A.; Akana, Y.; Ushida, Y.; Masuda, T.; Nakajima, A. Pure Appl Chem 1985, 57, 823.
65. Utracki, L.; Schlund, B. Polym Eng Sci 1987, 27, 367.
66. Dormier, E. J.; Tong, P. P.; Lagasse, R. G. Soc Plast Eng Tech Pap Annu Tech Conf 1984, 30, 421.
67. Wild, L.; Ranganath, R.; Knobeloch, D. C. Polym Eng Sci 1976, 16, 811.
68. Wong, C. M.; Shih, H. H.; Huang, C. J. Soc Plast Eng Tech Pap Annu Tech Conf 1997, 43, 1522.
69. Lachtermacher, M. G.; Rudin, A. J Appl Polym Sci 1996, 59, 1775.
70. Booij, H. C. Kautschuk Gummi Kunststoffe 1991, 44(2), 128.
71. Chambon, F. Soc Plast Eng Tech Pap Annu Tech Conf 1995, 41, 1157.
72. Haxlitt, L. G.; Karende, S. V.; Castille, M. J. J Appl Polym Sci 1994, 51, 271.
73. Raju, V. R.; Smith, G. G.; Marin, G.; Knox, J. R.; Graessley, W. W. J Polym Sci Polym Phys Ed 1979, 17, 1183.